24th COBEM - 2017

24th ABCM International Congress of Mechanical Engineering
December 3-8, 2017, Curitiba, PR, Brazil

COBEM-2017-2130
EFFECTS OF CRACK TUNNELING ON THE ELASTIC UNLOADING COMPLIANCE OF SE(B) SPECIMENS - CURRENT LIMITATIONS AND PROPOSALS

Leonardo Giangiulio Ferreira de Andrade [1,3]
[1] leonardogfa@gmail.com
Gustavo Henrique Bolognesi Donato [2,3]
[2] gdonato@fei.edu.br
[3] Centro Universitário FEI, Humberto de Alencar Castelo Branco Av., 3972,
São Bernardo do Campo, SP, ZIP 09850-901

Abstract. *This paper investigates the effects of crack tunneling on the elastic unloading compliance of SE(B) 1T fracture specimens. Numeric simulations were conducted with three levels of crack depth and five levels of crack curvature. Results show that for the same equivalent straight crack proposed by the ASTM E1820, the elastic compliance decreases with the increase of the crack front curvature, showing that the predicted crack size in real experiments would be smaller than the equivalent straight crack proposed by the ASTM. No significant deviations were detected within ASTM limits (ASTM, 2013a), which guarantees accurate crack size estimations if standardized requirements are met. When those limits are surpassed, on the other hand, significant deviations were found, and a new proposal for determining the equivalent straight crack in such situations was developed. The deviations provided by the new proposal were very reduced and tend to lead to a better understanding regarding the test of SE(B) specimens containing curved cracks.*

Keywords: *Fracture mechanics. Elastic unloading compliance. SE(B) specimen. Crack tunneling.*

1. INTRODUCTION

The use of high toughness structural materials is increasing within the industry. On top of that, understanding how cracks behave in these materials is critical for its use in high responsibility structures such as airplanes, gas pipelines and nuclear reactors. The procedures for the safe application of these materials are highly dependent on accurate resistance curves (*J-R* curves) (ASTM E1820, 2013a) and fatigue crack growth evolutions (*da/dN vs. ΔK*) (ASTM, 2013b), which represent the basis for structural integrity assessments (API 579, 2016; BS7910, 2013). Both aforementioned mechanical properties correlate driving force, which have consolidated calculation methods in ASTM standards, with instantaneous crack size *a*, calculated with real time techniques such as the elastic unloading compliance, electrical or optical methods.

Throughout fracture mechanics tests, load *P* and displacement *V* (which can be obtained from simple clip-gages and load cells) allow real-time stiffness computation. The increase of compliance *V/P* (the inverse of stiffness *P/V*) can be used to predict the instantaneous crack size *a* (Fig. 1) based on the elastic unloading compliance methodology, focus of this paper. However, several phenomena may affect compliance, for example: tridimensional effects, side-grooves, specimen rotation, closure, crack tip plasticity and tunneling. Focusing in the last one, tunneling happens when the central portion of the crack propagates faster than the edges. This occurs due the difference of stress triaxiality, which is more severe in the central portion, causing the crack to curve (ANDERSON, 2005).

ASTM standards establish limits for crack curvature to assure that it won't have any detrimental effects in terms of crack size and crack driving force (ASTM E1820, 2013a). To perform such validation, a post-mortem analysis of the specimen is required, in which the crack profile can be fully characterized. The problem faced here is that many real fracture specimens present crack curvatures (denoted here tunneling) higher than the allowed by ASTM and therefore need to be discarded, resulting in loss of financial resources and samples. This study evaluated numerically how tunneling affects compliance on SE(B) 1T specimens to assess if ASTM assumption is reasonable. In addition, the paper presents proposals to the cases where ASTm requirements are violated and errors remarkable.

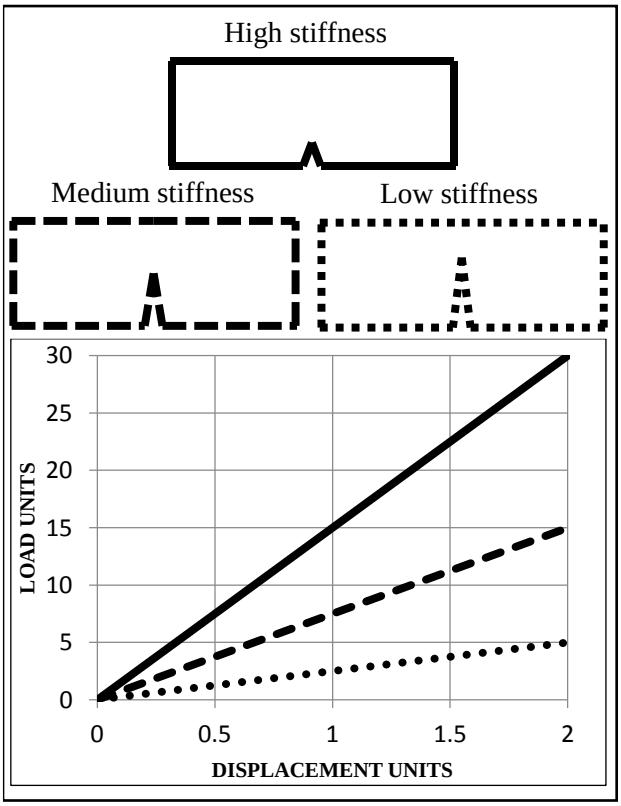

Figure1. Example of elastic compliance correlation with crack depth.

2. THEORETHICAL BACKGROUND

In this section, the ASTM straight crack criteria and previous studies on how tunneling impacts the elastic unloading compliance will be revised.

2.1 ASTM equivalent straight crack

According to ASTM E1820 (2013a), the physical measuring of the initial, final and intermediate crack sizes should be done after the test has ended and the two pieces of the specimen are separated. The crack should be measured in nine equidistant points, with one in the center and two at 0.005W of the edges of the specimen. Then, the average of the two points closer to the edges is calculated and finally, the arithmetical average of the remaining eight values determines the average crack size. The equivalent straight crack can also be determined in terms of relative crack depth for convenience, and it is shown below:

$$a/W_{eq.} = \frac{\frac{(a/W_1 + a/W_9)}{2} + a/W_2 + a/W_3 + a/W_4 + a/W_5 + a/W_6 + a/W_7 + a/W_8}{8}, \quad (1)$$

where:

a/W_{eq}: equivalent relative crack depth;

a/W_i: relative crack depth at the nine points of measurement indicated by ASTM E1820 [1].

If the crack is symmetrical, $a/W_1 = a/W_9$, $a/W_2 = a/W_8$, $a/W_3 = a/W_7$ and $a/W_4 = a/W_6$ leading to:

$$a/W_{eq.sim} = \frac{\frac{(2a/W_1)}{2} + 2a/W_2 + 2a/W_3 + 2a/W_4 + a/W_5}{8}, \tag{2}$$

and therefore:

$$a/W_{eq.sim} = 0.125\,a/W_1 + 0.250\,a/W_2 + 0.250\,a/W_3 + 0.250\,a/W_4 + 0.125\,a/W_5. \tag{3}$$

The coefficients from Eq. (3) (denoted here β) are now defined as the weights each measurement impacts on the equivalent crack size. For the ASTM E1820 (2013a) and assuming symmetrical crack, $\beta_1 = \beta_5 = 0.125$ (center and edges) and $\beta_2 = \beta_3 = \beta_4 = 0.250$ (intermediate points).

2.2 Tunneling effects on compliance

Several studies investigated the problem of tunneling yielding undesirable results in compliance. To obtain precise fracture mechanics data that is dependent of the crack size, a straight crack front is desirable, which represents constant crack size throughout the crack. However, due to a predominant triaxial stress state in the center of a specimen and a plane stress condition on the edges, a crack tends to be more severely loaded in the center portion, causing it to grow deeper in that region (ANDERSON, 2005).

Steenkamp (1988) is among the first to publish a study about tunneling effects on compliance on SE(B) specimens. It was used a bi-dimensional finite element model with plane stresses to describe the whole SE(B) specimen, which is not true once the center portion is under a triaxial stress state. The results showed a decrease in compliance as the curvature rose.

Knowing the limitations of the analysis conducted by Steenkamp, further studies have proven to be necessary. Yan and Zhou (2014) also studied tunneling effects on compliance for SE(B) specimens, but with a highly refined finite element mesh. This study concluded that within the ASTM limits, less the 1% of deviation of the compliance due to tunneling was observed, showing that the ASTM criteria is valid. Further study was also done on the SE(T) specimen by Huang and Zhou (2015). Similar conclusions as for the SE(B) (YAN and ZHOU, 2014) were found, once again proving that the ASTM criteria is valid since its requirements are met.

Both Yan and Zhou (2014) and Huang and Zhou (2015) studies considered a crack curvature as defined by Nikishkov, Heerens and Hellmann (1999). Based on the observation of 198 C(T) specimens, a crack curvature equation was developed and served as basis for the aforementioned studies. The present work, however, did not use the description of the crack front as proposed by Nikishkov, Heerens and Hellmann (1999), and the crack curved front was modeled as a semi-ellipse – the reason is that initial validations conducted by current authors proved that this approach presented very similar trends and effects (both qualitative and quantitatively) if compared to the aforementioned approach.

3. METHODOLOGY

3.1. Materials and constitutive laws

Since plasticity is not involved in this study, it was considered an elastic material with *E=206 GPa* and *v=0.3*. That is enough to represent high toughness steels in linear elastic regimen isolating tunneling effects.

3.2 Geometry

SE(B) specimens are the subject of this work. 1T geometry configuration was studied, which means thickness is *B=25.4 mm*, width *W=50.8 mm* and span *S=4.W*. Three values of crack depths were used to represent a shallow, medium and deep crack and were shown as relative crack depths of *a/W=0.2*, *a/W=0.5* and *a/W=0.7*. A tunneling level parameter *T* was developed to describe the crack curvature, which can be calculated as shown below:

$$T = \max(a/W_i) - \min(a/W_i). \tag{4}$$

As previously explained, crack front was modeled as a semi-ellipse, with its main dimensions in accordance to the literature (YAN and ZHOU, 2014, HUANG and ZHOU, 2015). Five levels of tunneling were incorporated to the refined finite element models by distorting the original straight crack mesh of the virtual SE(B) specimen with a Matlab algorithm ensuring that the equivalent straight crack calculated by the ASTM proposal was the original crack depth before any modification to the mesh. Tunneling levels were *0, 1 mm, 2 mm, 4 mm* and *6 mm*.

3.3 Finite Element (FE) models

The adequate development of the FE models is key to reach the main objective of this research. Element type and mesh size affects results and simulation process time, and for that reason a convergence analysis was necessary. Huang and Zhou (2015) utilized a highly refined 3-D mesh with 20-node hexahedral elements while Moreira (2013) also used a highly refined 3-D mesh but with 8-node hexahedral elements. It was determined by the author that for linear elastic simulations and considering refined meshes, 8-node elements were just as accurate as the 20-node elements with less simulation process time. A highly refined mesh (6000-8000 elements and 7000-9000 nodes) based on 8-node hexahedral elements was chosen to implement the models. 10 elements with linearly varying thickness were used to describe the semi-thickness of the models, since they are symmetric. An example of a model used in this paper is shown in Figure 2 without and with induced tunneling.

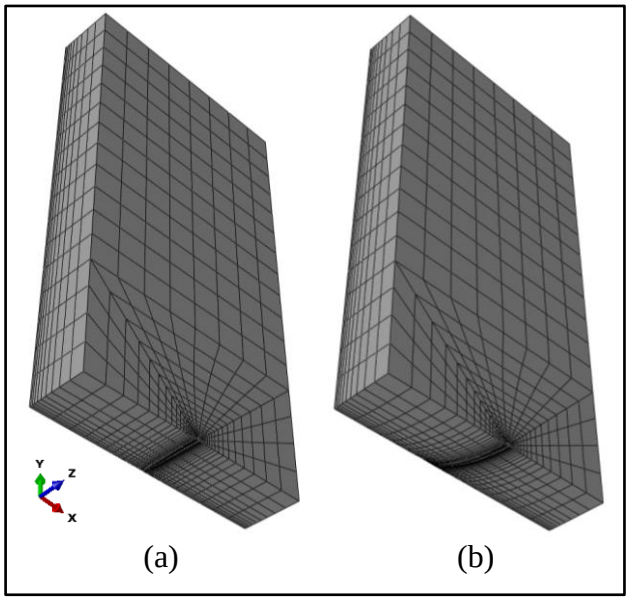

Figure 2. Example of a SE(B) model. One quarter of the specimen is modeled following adequate boundary conditions. (a) Straight crack. (b) Curved crack.

The mesh was then built starting with a *"spider-web"* mesh with *0.05mm* of radius to represent the crack tip. No differences in results were observed when compared to smaller values of crack tip radius such as *0.005mm* and *0.0005mm*, both with higher simulation time. This crack front description is in accordance to the literature (VERSTRAETE, 2014). MSC Patran was the pre-processor of choice. One quarter of the specimens was modeled to save simulation time. Usual boundary conditions were applied to ensure proper loading and symmetry.

3.4 Loading

Loading to the specimen was simulated by a total displacement of 0.2 mm imposed in the LLD (Load Line Displacement – Δ – see Fig. 3) plane, since linear elastic constitutive model was adopted to the material. No unloading was necessary since the behavior of loading and unloading must be the same under such conditions. For all models representing the SE(B) specimens, the nodes of the crack plane that were coincident to the loading point (Δ,*P* in Fig. 3) were chosen to represent the upper roller of a three point bend apparatus.

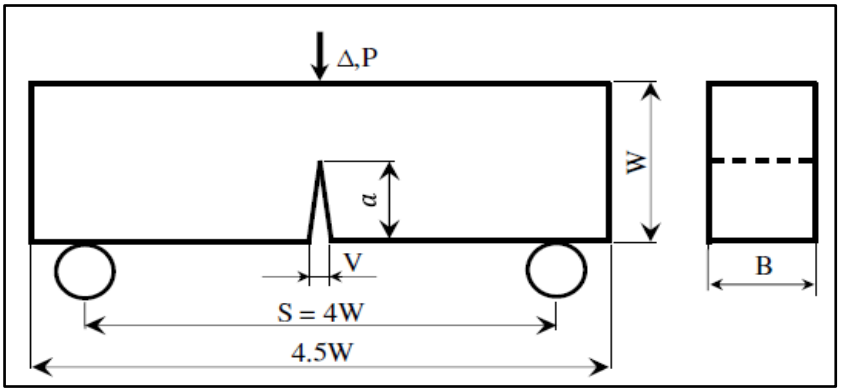

Figure 3. Main dimensions and load strategy of SE(B) specimens. For 1-T geometries, W=2B and B = 25.4 mm.

4. RESULTS

Based on the finite element results in terms of loads (*P*) and respective displacements (in special CMOD – *V*), the compliances could be quantified and the following results emerged (Figure 4). It is displayed the evolution of compliance (*y* axis - continuous line) as a function of tunneling level (*x* axis - *T*). The ASTM limit is represented by a dashed vertical line. C_{DELTA} is the percentage variation of compliance, calculated as:

$$C_{DELTA} = \left(\frac{C - C_0}{C_0} \right).100, \tag{5}$$

where C_0 is the compliance for a straight crack (T = 0).

It was realized a minimum influence of crack curvature within ASTM limits for the three crack depths (below ~ 0.5%), but a much more severe impact when those limits are violated with maximum compliance decrease ranging from -3.72% up to -5.95% for *T* = 6 mm, which can influence crack size predictions when using elastic unloading compliance technique. Those results are in accordance with the literature (STEENKAMP, 1988; YAN and ZHOU, 2014; HUANG and ZHOU, 2015). Detailed results are shown below in Tables 1-3.

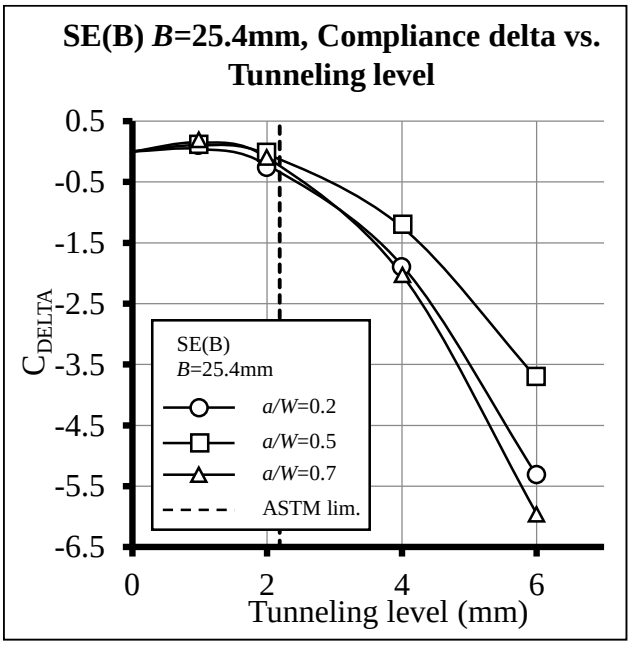

Figure 4. Compliance evolution for SE(B) 1T. All three crack depths were evaluated.

Tab. 1. Detailed results for the SE(B) 1T *a/W*=0.2.

T (mm)	**C (mm/N.10^{-6})**	**C$_{DELTA}$ (%)**	**Predicted *a/W***	***a/W*$_{DELTA}$ (%)**
0	1.319	0	0.196	0
1	1.319	0.04	0.196	0.03
2	1.316	-0.22	0.196	-0.18
4	1.294	-1.87	0.193	-1.56
6	1.248	-5.32	0.187	-4.49

Tab. 2. Detailed results for the SE(B) 1T *a/W*=0.5.

T (mm)	**C (mm/N.10^{-6})**	**C$_{DELTA}$ (%)**	**Predicted *a/W***	***a/W*$_{DELTA}$ (%)**
0	6.557	0	0.493	0
1	6.564	0.10	0.493	0.04
2	6.555	-0.04	0.493	-0.02
4	6.476	-1.24	0.491	-0.46
6	6.313	-3.72	0.486	-1.40

Tab. 3. Detailed results for the SE(B) 1T *a/W*=0.7.

T (mm)	**C (mm/N.10^{-6})**	**C$_{DELTA}$ (%)**	**Predicted *a/W***	***a/W*$_{DELTA}$ (%)**
0	23.458	0	0.693	0
1	23.493	0.15	0.693	0.03
2	23.435	-0.10	0.693	-0.02
4	22.983	-2.02	0.691	-0.39
6	22.061	-5.95	0.685	-1.17

Knowing that a severe impact can occur when the ASTM limits are violated, a new proposal based only on geometry, was developed. The key factor was developing an equation capable of predicting the position of a straight equivalent crack that would yield the same compliance as the curved one. That could be achieved making this equation function of the tunneling level *T*, as shown for a symmetrical crack in Equation 6 and Table 4 for an example of SE(B) specimen with *a/W = 0.7*. Finite elements analyses of several specimens with varying crack offsets were conducted to find the optimal position of the crack, and then with optimization techniques the results displayed below in Table 4 were achieved.

$$a/W_{eq.sim} = \beta_1 a/W_1 + \beta_2 a/W_2 + \beta_3 a/W_3 + \beta_4 a/W_4 + \beta_5 a/W_5 \quad (6)$$

Table 4. Group of β coefficients for all tunneling levels considered for the SE(B), B=25.4mm a/W=0.7 written as function of the tunneling level T.

β coefficients, SE(B) B=25.4mm a/W=0.7	
β_1 = -0.0051T + 0.1462	(center)
β_2 = -0.0096T + 0.2230	
β_3 = -0.0203T + 0.3227	
β_4 = 0.0193T + 0.2139	
β_5 = 0.0157T + 0.0943	(edge)

The comparison between the ASTM predictions and the new proposal are shown below in Figure 5, and a major reduction in the C_{DELTA} was detected for every evaluated tunneling level. The deviations (C_{Delta}) considering the new proposal is comparable - while slightly better - than ASTM predictions inside ASTM's validity limits. However, when such limits are violated, the new proposal represents much lower deviation, unde ± 0.5 % even for severe tunneling of T = 6 mm. Despite further experimental validations and the study of respective crack driving forces are necessary, these results call thet attentions for the possibility of expanding the validity of fracture and fatigue specimens based on SE(B) geometries.

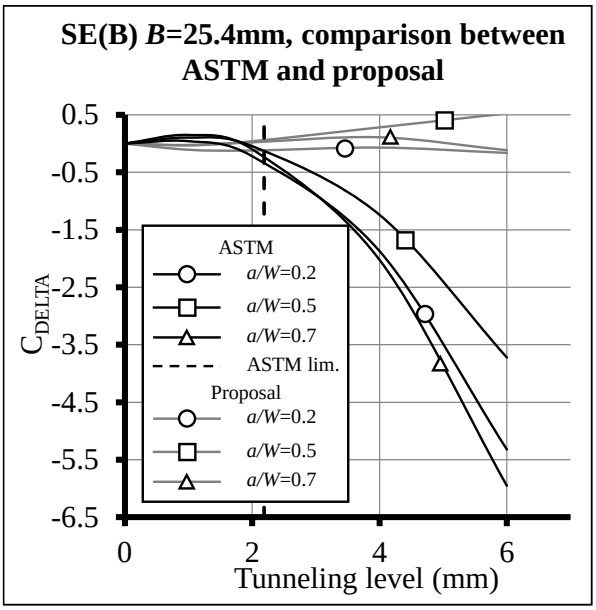

Figure 5. Compliance evolution for SE(B) 1T specimens. All three crack depths were evaluated. In black: ASTM. In Grey: Current proposal.

5. CONCLUDING REMARKS

The main objective of describing how the compliance behaves with increasing curvature was achieved. Figure 4 shows that compliance will increase slightly and then decrease severely with the increase of tunneling level T.

Tunneling within ASTM E1820 limits do not generate significant deviations in compliance (under ± 0.5%), showing that the standardized criterion is robust if its requirements are met.

On the other hand, tunneling levels beyond the standard limits generate severe deviations when comparing the compliance of tunneled samples to the compliance of samples containing straight cracks. It represents the loss of several samples during real tests or, if not detected, a risk for the accuracy of fatigue and fracture mechanics testing.

New solutions for equivalent straight cracks were developed and proposed for the SE(B) geometry. The proposal reveals reduced deviations when compared to ASTM statements. Despite that, experimental validations and the study of the respective crack driving forces are being developed for further understanding of the tunneled crack behavior.

6. ACKNOWLEDGEMENTS

This investigation is supported by the Brazilian Council for Scientific and Technological Development - CNPQ (grant 486176/2013-4), by the Coordination for the Improvement of Higher Education Personnel - CAPES and by Centro Universitário FEI, Brazil, through the use of its laboratories and human resources.

7. REFERENCES

AMERICAN PETROLEUM INSTITUTE - API, "Fitness-For-Service", API 579-1 / ASME FFS-1, 3rd ed., 2016.

AMERICAN SOCIETY FOR TESTING AND MATERIALS. ASTM E1820: Standard Test Method for Measurement of Fracture Toughness, Philadelphia, 2013a.

AMERICAN SOCIETY FOR TESTING AND MATERIALS. ASTM E647: Standard Test Method for Measurement of Fatigue Crack Growth Rates, Philadelphia, 2013b.

ANDERSON, T. L. Fracture mechanics. 3. ed. New York: Taylor & Francis Group, 2005.

BRITISH STANTARDS INSTITUTE - BSI, "Guide to methods for assessing the acceptability of flaws in metallic structures", BS 7910:2013 + A1:2015, 2013.

HUANG, Y.; ZHOU, W. Effects of crack front curvature on J-R curve testing using clamped SE(T) specimens of homogeneous materials. International Journal of Pressure Vessels and Piping, n. 134, p. 112-127, 2015.

MOREIRA, F. C.; DONATO, G. H. B. Effects of side-grooves and 3-D geometries on compliance solutions and crack size estimations applicable to C(T), SE(B) and clamped SE(T) specimens. Proceedings of the ASME 2013 pressure vessels & piping division. Paris, France, 2013.

NIKISHKOV, G.; HEERENS, J.; HELLMANN, D. Effect of crack front curvature and side grooving on CTOD δ5 and J-integral in CT and 3PB specimens. Journal of Testing and Evaluation, JTEVA, v. 27, n. 5, p. 312-319. set.1999.

STEENKAMP, P. JR-curve testing of three-point bend specimens by the unloading compliance method. Fracture Mechanics: Eighteenth Symposium, ASTM STP 945, p. 583-610. Philadelphia, 1988.

YAN, Z.; ZHOU, W. Effect of crack front curvature on CMOD compliance and crack length evaluation for single-edge bend specimens. Proceedings of the Canadian society for mechanical engineering international congress, 2014.

VERSTRAETE, M. A. et al. Evaluation and interpretation of ductile crack extension in sent specimens using unloading compliance technique. Engineering Fracture Mechanics, v. 115, p. 190-203. 2014.

WU, S. X. Crack length calculation formula for three point bend specimens. Interna-tional Journal of Fracture, v. 24, p. R33-R35. 1984.

8. RESPONSIBILITY NOTICE

The authors are the only responsible for the printed material included in this paper.